RNA (2000), *6*:628–637. Cambridge University Press. Printed in the USA.

Intracellular ribozyme-catalyzed *trans*-cleavage of RNA monitored by fluorescence resonance energy transfer

DANIELLE VITIELLO, DAVID B. PECCHIA, and JOHN M. BURKE

Markey Center for Molecular Genetics, Department of Microbiology and Molecular Genetics, The University of Vermont, Burlington, Vermont 05405, USA

ABSTRACT

Small catalytic RNAs like the hairpin ribozyme are proving to be useful intracellular tools; however, most attempts to demonstrate *trans*-cleavage of RNA by ribozymes in cells have been frustrated by rapid cellular degradation of the cleavage products. Here, we describe a fluorescence resonance energy transfer (FRET) assay that directly monitors cleavage of target RNA in tissue-culture cells. An oligoribonucleotide substrate was modified to inhibit cellular ribonuclease degradation without interfering with ribozyme cleavage, and donor (fluorescein) and acceptor (tetramethylrhodamine) fluorophores were introduced at positions flanking the cleavage site. In simple buffers, the intact substrate produces a strong FRET signal that is lost upon cleavage, resulting in a red-to-green shift in dominant fluorescence emission. Hairpin ribozyme and fluorescent substrate were microinjected into murine fibroblasts under conditions in which substrate cleavage can occur only inside the cell. A strong FRET signal was observed by fluorescence microscopy when substrate was injected, but rapid decay of the FRET signal occurred when an active, cognate ribozyme was introduced with the substrate. No acceleration in cleavage rates was observed in control experiments utilizing a noncleavable substrate, inactive ribozyme, or an active ribozyme with altered substrate specificity. Subsequently, the fluorescent substrates were injected into clonal cell lines that expressed cognate or noncognate ribozymes. A decrease in FRET signal was observed only when substrate was microinjected into cells expressing its cognate ribozyme. These results demonstrate *trans*-cleavage of RNA within mammalian cells, and provide an experimental basis for quantitative analysis of ribozyme activity and specificity within the cell.

Keywords: catalytic RNA; FRET; hairpin; mammalian cells

INTRODUCTION

Engineered ribozymes possess broad potential as tools for targeted RNA inactivation in diverse organisms, ranging from plants to humans (Christoffersen & Marr, 1995). *Trans*-acting ribozymes are well suited for targeted RNA cleavage as they function without protein cofactors and can be expressed within or delivered to cells. Cellular applications of ribozyme technology have centered around three classes of ribozymes: hammerhead (Birikh et al., 1997; Rossi, 1997); hairpin (Burke, 1996; Earnshaw & Gait, 1997; Yu et al., 1998); and group I ribozymes (Sullenger & Cech, 1994; Jones et al., 1996; Jones & Sullenger, 1997; Kohler et al., 1999). Over the past 10 years, dramatic advances have been made in our understanding of the structure and in vitro activity of ribozymes.

In contrast, success in using ribozymes to inhibit the expression of targeted genes has been mixed. Little correlation can be drawn between activity in vitro versus activity in vivo. *Trans*-acting hammerhead ribozymes unable to cleave short oligoribonucleotide fragments of HIV RNA in simple buffers were able to decrease HIV RNA levels when expressed intracellularly (Crisell et al., 1993; Steinecke et al., 1994; Domi et al., 1996). Other reports have demonstrated that hairpin (Chowrira et al., 1994; Welch et al., 1996) and hammerhead (Bertrand et al., 1994; Sun et al., 1994; Lieber & Strauss, 1995) ribozymes had similar activity in the test tube and in cell culture, whereas other laboratories have found that ribozymes that are active in vitro show no effect on gene expression in vivo.

There are several plausible reasons for this mixed success in vivo. We have recently shown that target-site

Reprint requests to: John M. Burke, Microbiology and Molecular Genetics, The University of Vermont, 306 Stafford Hall, Burlington, Vermont 05405, USA; e-mail: John.Burke@uvm.edu.

occlusion is likely to be a major reason why hairpin ribozymes can fail to cleave long, biological RNA molecules, and have developed a combinatorial activity-based selection method to identify the sites in a structured RNA target that may be cleaved most efficiently (Yu et al., 1998). It is also possible that intracellular *trans*-cleavage activity of ribozymes is lower than one would expect based on in vitro studies. In this regard, it should be noted that the intracellular concentration of free magnesium (~1 mM) is approximately 10-fold lower than used for most in vitro studies (~10 mM) (Schoolwerth et al., 1997).

It is important that accurate and quantifiable methods be developed for the analysis of intracellular *trans*-cleavage activity. Studies to date have suffered from two major complications. First, the RNA cleavage products appear to be degraded rapidly by cellular nucleases and thus are not amenable to analysis. Second, both hairpin and hammerhead ribozymes can cleave their substrates after cellular lysis, during RNA extraction and analysis (Beck & Nassal, 1995; Heidenreich et al., 1996). A few studies have controlled for ribozyme cleavage during cellular extraction, while convincingly demonstrating *cis*-acting ribozyme-mediated intracellular cleavage in plants (Borneman et al., 1995), in yeast (Donahue & Fedor, 1997), and in mammalian cells (Chowrira et al., 1994; Seyhan et al., 1998).

In this article, we directly demonstrate intracellular hairpin ribozyme activity in individual living cells. A fluorescence assay previously utilized to examine RNA structure and oligonucleotide integrity (Sixou et al., 1994; Perkins et al., 1996; Uchiyama et al., 1996; Walter et al., 1998) has been adapted to monitor ribozyme catalysis in vivo. Fluorescence resonance energy transfer (FRET) involves the nonradiative transfer of energy from a donor (fluorescein) to an acceptor (tetramethylrhodamine) fluorophore (Clegg, 1992; Perkins & Goodchild, 1997). In this study, an acceptor-donor fluorophore pair was introduced into the substrate RNA at positions flanking the cleavage site. Substrate cleavage and subsequent product dissociation disrupts energy transfer, resulting in a red-to-green shift in the dominant emission spectrum that can be measured both in simple buffers and in cells. Our results demonstrate that ribozyme catalysis can be visualized in cells through FRET.

RESULTS

Ribozyme activity and stability

A well-studied variant of the hairpin ribozyme was used for these studies (Esteban et al., 1997). It was modified by the introduction of flanking 5′- and 3′-stem-loop structures (Fig. 1) to inhibit degradation by cellular exonucleases. These flanking structures did not significantly diminish catalytic activity in assays using short, synthetic substrates (Table 1). Electrophoretic analysis of the modified and unmodified ribozymes in 10% human serum demonstrated that the stem-loop structures were effective in increasing the stability of the ribozyme against ribonucleases (data not shown). Results showed that exonucleases removed unstructured 3′ terminal sequences, stopping at or near the base of the flanking stem. The resulting ribozymes retained effective catalytic activity with single-turnover cleavage rates decreased by only 50% (data not shown).

Two control ribozymes were also synthesized. An inactive ribozyme that retains substrate-binding activity was generated by introducing two base substitutions, G_8A and G_{21}U (Berzal-Herranz et al., 1993). This ribozyme construct was used to examine the potential effects of antisense binding. To examine the specificity of the ribozyme, we altered the sequence of the substrate-binding strand, changing one base in helix 1 ($U_4 \rightarrow$ C) and two bases in helix 2 ($G_{13} \rightarrow$ A, $C_{12} \rightarrow$ G) such that the ribozyme could no longer bind substrate.

Stabilized fluorescent oligoribonucleotide substrates

A series of substrate modifications were made to increase the substrate's resistance to cellular nucleases while maintaining its ability to be cleaved by the ribozyme (Table 1). Half-lives of the modified substrates were measured in 10% human serum, supplemented as described (Beigelman et al., 1995). A G_{+1}A noncleavable substrate analog was modified in a manner identical to that of the cleavable species; this analog can bind to the ribozyme with nearly the same affinity as normal substrate, but will not be cleaved (Chowrira et al., 1991; Walter et al., 1997). Substrate stability was tested by incubating 5′-radiolabeled substrates in standard cleavage buffer supplemented with 10% human serum and analyzed by denaturing gel electrophoresis. Nucleases degraded the 5′ radioactively labeled synthetic, unmodified substrate to completion within 30 s. To enhance stability, we incorporated 2′O-methyl ribonucleotides during synthesis (Table 1). These modifications resulted in a sixfold increase in nuclease resistance, with a relatively small (twofold) decrease in cleavage rate by the ribozyme (Table 1).

Further enhancement of nuclease resistance was achieved through the introduction of thiophosphates at the ultimate and penultimate phosphate moieties, in addition to the 2′ O-methyl ribonucleotides. These additional modifications had little or no effect on cleavage rate, but further improved nuclease resistance.

The length of the substrate was extended to include donor and acceptor fluorophores and 2′ O-methyl ribonucleotides with thiophosphate linkages at the flanking ends (Fig. 1). The fluorescein phosphoramidite and an amino-linker were incorporated during solid-phase phosphoramidite synthesis. Following synthesis, an

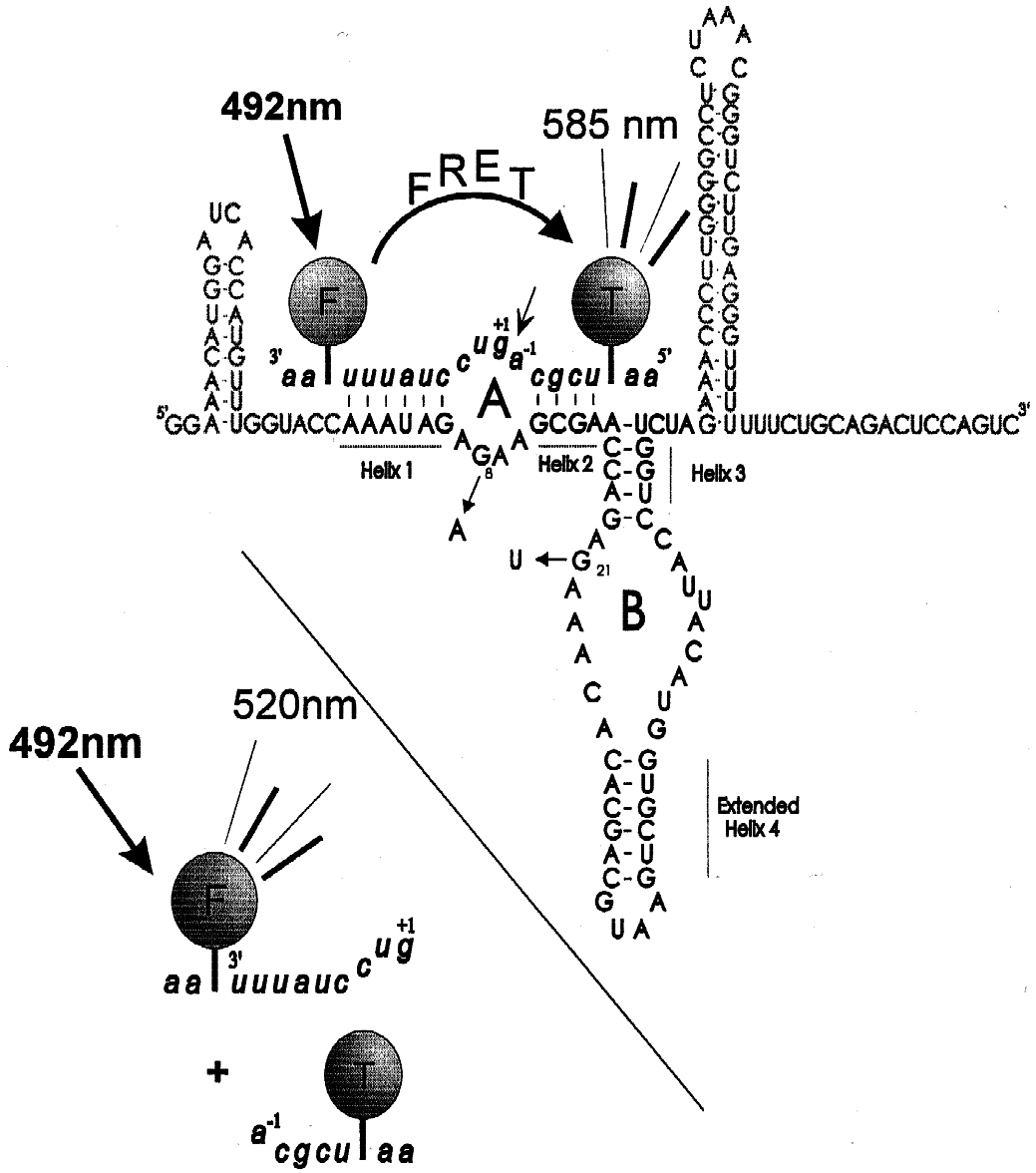

FIGURE 1. Hairpin ribozyme and fluorescent substrate. Ribozyme and substrate sequences are in uppercase and lowercase letters, respectively. The 5′ and 3′ flanking stem-loops (MacDonald et al., 1993; Sargueil et al., 1995) are gray. The ribozyme sequence (Esteban et al., 1997) is indicated in bold lettering; F is fluorescein and T is tetramethylrhodamine coupled to a C_6-amino linker. The arrow indicates the substrate-cleavage site. G_8A and $G_{21}U$ render the ribozyme inactive, but still able to bind substrate with a K_d comparable to that of the active species (Berzal-Herranz et al., 1993). **Lower left:** cleavage of substrate results in product dissociation and FRET decay.

amine-reactive succinylmidyl ester of tetramethylrhodamine was coupled manually to the amino-linker on the oligonucleotide. Single-turnover cleavage assays showed that the double-labeled substrate was cleaved with kinetics similar to that of its nonlabeled counterpart (Table 1).

In vitro FRET activity was measured by simultaneously recording emission at 520 nm and 585 nm (Fig. 2A) using a continuous 492-nm excitation source. Substrate and ribozyme were preincubated separately at 37 °C. Prior to ribozyme addition, FRET resulted in a tetramethylrhodamine emission intensity (5.2 U) twice that of fluorescein. Substrate cleavage following the addition of a 20-fold molar excess of ribozyme caused an inversion of the fluorescence ratio as fluorescein became the dominant emitting fluorophore within 10 min. The corresponding tetramethylrhodamine signal decreased by one unit. Under these conditions, equilibrium of the acceptor-to-donor intensity ratio (0.6) was reached within 20 min.

Changes in FRET decay were demonstrated through a variable emission scan (500–650 nm) at a fixed excitation wavelength (492 nm) before and after ribozyme addition, corresponding to initial and final timepoints

TABLE 1. Modified ribonucleotides increase substrate stability.

Substrate	k_{cleave} (min^{-1})	*t* (min)
$^{5'}$UCGCA^{-1}/G^{+1}UCCUAUUU	0.4	<1
UCGCA/**A**UCCUAUUU	0.0[a]	<1
UCGCA/GUCCUAUUU	0.18	6.6[b]
UCGCA/GUCCUAUUU	0.10	6.6[b]
UCGCA/GUCCUAU***UU***	0.16	7.0[b]
AATUCGCA/GUCCUAUUU**FAA**	0.15/0.16[c]	N.D.

Underlined bases indicate 2′O-methyl ribonucleosides. Italicized bases indicate ribonucleoside phosphorothioates. T and F indicate tetramethylrhodamine and fluorescein. N.D.: not determined. *t* (min) represents the half-life of the substrates in 10% human serum, supplemented as described (Beigelman et al., 1995).

[a]The $G_{+1}A$ substitution renders the substrate uncleavable, but does not inhibit binding (Chowrira et al., 1991; Walter et al., 1997).

[b]The 5′-radioactive label was removed by phosphatase activity in addition to nucleolytic degradation. At incubations greater than 5 min, an additional band was seen on denaturing PAGE that migrated faster than a nucleoside monophosphate. The total signal from full-length and truncated products decreased with time.

[c]The cleavage rate for this substrate was calculated under single-turnover conditions by PhosphorImager analysis (Esteban et al., 1997) of the radiolabeled substrates, as well as by FRET, resulting in essentially identical cleavage rates (0.15 min^{-1} and 0.16 min^{-1}, respectively).

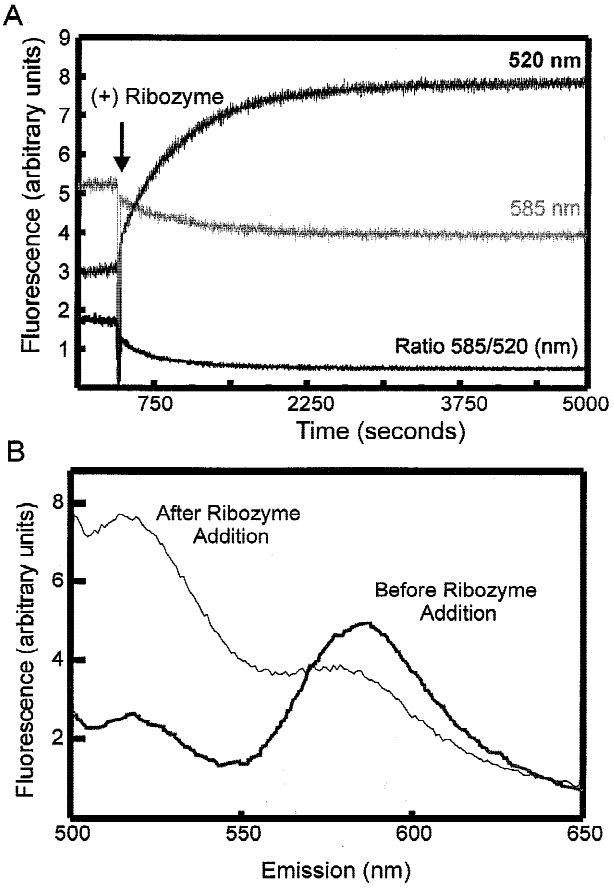

FIGURE 2. FRET analysis of ribozyme cleavage in simple buffers. Fluorescence was reported in arbitrary units. **A**: Simultaneous emission scans were obtained at 520 nm (fluorescein) and 585 nm (tetramethylrhodamine) with excitation at 492 nm, and the ratio of acceptor to donor fluorescence was calculated (see Materials and Methods). The inverted spike is a fluorometer artifact that occurred when the cuvette was exposed to light during addition of ribozyme to initiate the reaction. **B**: Emission scans were obtained at timepoints corresponding to the start and the end of the experiment in **A**. Substrate cleavage resulted in a shift from acceptor-dominant to donor-dominant species.

(Fig. 2B). Dissociation of the 5′- and 3′-cleavage products from the ribozyme resulted in a loss of FRET and a shift in dominant emission spectrum from tetramethylrhodamine (585 nm) to fluorescein (520 nm).

Control studies were performed to rule out the possibility that binding of substrate to the ribozyme might cause FRET decay. First, dual emission experiments were repeated, employing a $G_{+1}A$ substrate analog and a 20-fold molar excess of cognate, active ribozyme (Fig. 3C). This analog has been shown by fluorescence quenching to bind to the ribozyme with an apparent K_d of 310 pM (compared to 210 pM for the normal sequence) (Walter et al., 1997), but it does not mediate stable interaction between the ribozyme domains, and is not cleaved to detectable levels (Walter & Burke, 1997). A second control utilized the cleavable substrate and a 20-fold molar excess of cognate, but inactive ribozyme (G_8A, $G_{21}U$) (data not shown). Results in each case were the same. Formation of the ribozyme-substrate complex was accompanied by a 0.4-unit increase in fluorescein emission and a 0.2-unit decrease in the FRET ratio. The tetramethylrhodamine-emission spectrum did not change. Previous work in our laboratory has shown that fluorescein emission can be quenched by a specific interaction between the fluorophore and a nearby guanosine in RNA (Walter & Burke, 1997; Walter et al., 1997). In that work, a fluorescein at the 3′ end of the substrate molecule was quenched upon binding to a substrate-binding strand of the ribozyme that included an overhanging 5′ guanosine (necessary for T7 transcription). This ribozyme construct does not contain a guanosine close to the substrate fluorescein; indeed, the small increase in fluorescein emission upon binding might represent a slight dequenching, possibly preventing intramolecular interaction with a G in the substrate. These controls show that loss of the FRET signal (Fig. 2) correlates with ribozyme-mediated cleavage, and not the formation of the ribozyme-substrate complex.

The study of intracellular FRET decay involves the introduction of substrate and ribozyme into individual cells through microinjection of a solution containing both substrate and ribozyme, affording cellular colocalization while only breaching the membrane once. A further advantage of coinjection is that the ratios of ribozyme to substrate are maintained at a constant level. Divalent cations, preferably magnesium (>3 mM), are essential for ribozyme activity at low ionic strength

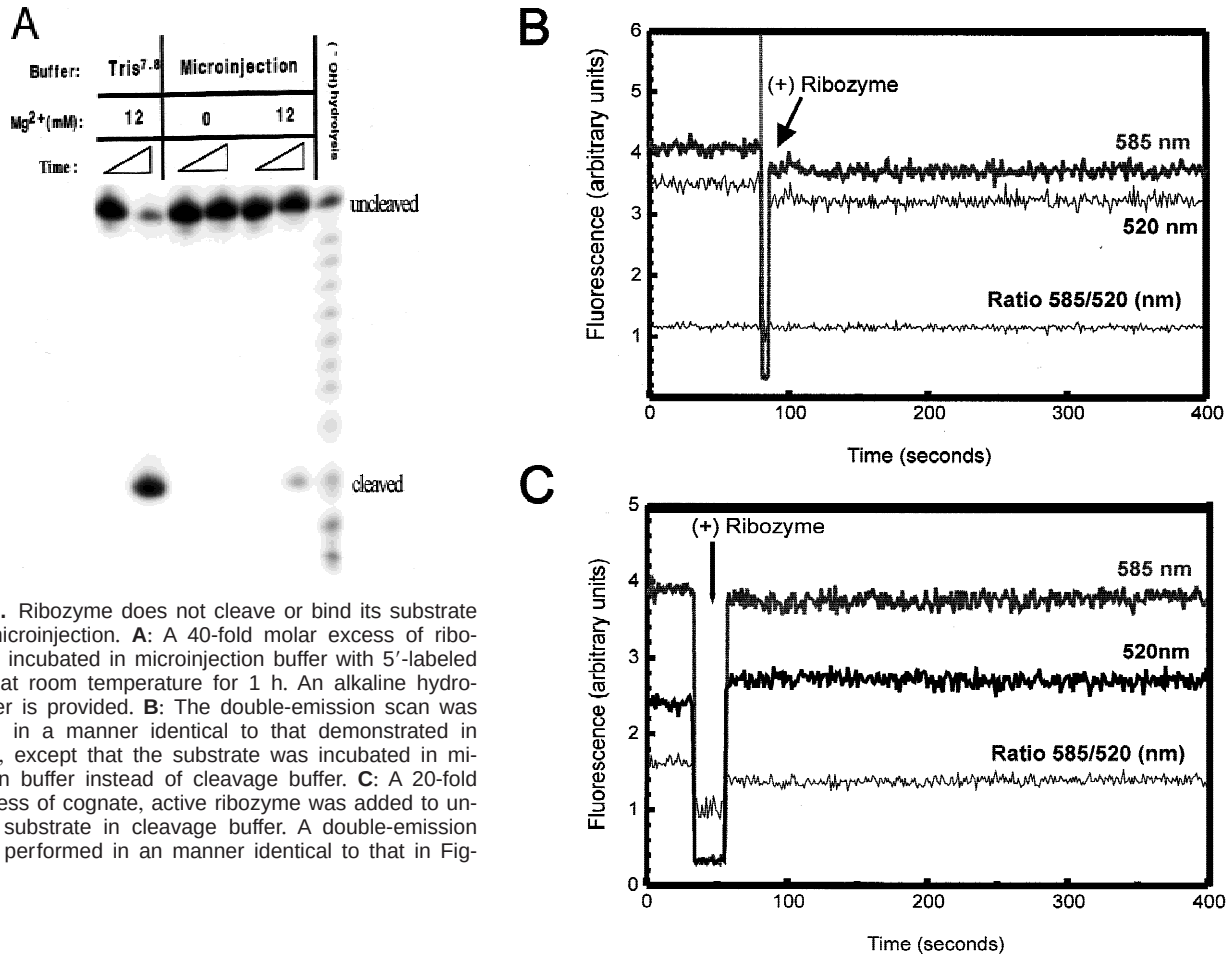

FIGURE 3. Ribozyme does not cleave or bind its substrate prior to microinjection. **A**: A 40-fold molar excess of ribozyme was incubated in microinjection buffer with 5′-labeled substrate at room temperature for 1 h. An alkaline hydrolysis ladder is provided. **B**: The double-emission scan was performed in a manner identical to that demonstrated in Figure 2A, except that the substrate was incubated in microinjection buffer instead of cleavage buffer. **C**: A 20-fold molar excess of cognate, active ribozyme was added to uncleavable substrate in cleavage buffer. A double-emission scan was performed in an manner identical to that in Figure 2A.

(Chowrira et al., 1993). To confirm that substrate binding and cleavage can occur only within the cell, a radioactively labeled synthetic substrate was incubated with a 40-fold molar excess of ribozyme in magnesium-free microinjection buffer [10 mM NaH_2PO_4/ Na_2HPO_4 (pH 7.2), 70 mM KCl] at room temperature for 1 h (Fig. 3A). No cleavage products were observed. However, addition of Mg^{+2} to 12 mM restored ribozyme activity. Relative FRET efficiency (Fig. 3B) did not change when a 20-fold excess of ribozyme was added to substrate in microinjection buffer. When the ribozyme–substrate complex forms, it produces an immediate shift in the acceptor-to-donor ratio (Fig. 3C) that did not occur when ribozyme was added to substrate in microinjection buffer. However, when Mg^{+2} was added to 12 mM, ribozyme cleaved its substrate as evidenced by loss of FRET signal (data not shown). These controls indicate that the ribozyme activity visualized in the microinjection experiments occurred within the cells.

FRET analysis of intracellular *trans*-cleavage

Cytosolic microinjection of adherent OST-7 cells or BHK-21 cells was performed under light transmission; 30–50 cells were injected per experiment. Cells were exposed to the fluorescent light source only after microinjection was complete (20–60 s), thereby minimizing the photobleaching of the fluorophores.

Changes in relative FRET efficiency were monitored by manual switching of the excitation filters. Following microinjection, cells were illuminated with UV light using a 470–490 nm filter and photographed to measure fluorescein fluorescence. Subsequently, tetramethylrhodamine fluorescence was photographed using cells illuminated through a 540–560 nm filter. Red fluorescence is expected upon 540–560 nm excitation in all cases, as the tetramethylrhodamine fluorophore is excited directly. In contrast, green fluorescence of fluorescein will only be observed after substrate cleavage, as energy transfer via FRET prevents radiative emission in uncleaved substrates.

When substrate alone was injected into OST-7 cells and excited (470–490 nm), there was no evidence of green fluorescence, indicating strong FRET by the acceptor fluorophore (Fig. 4, lower right). When excited with 540–560 nm light, tetramethylrhodamine emission was immediate and faded to background levels after approximately 7 min of continuous irradiation. Similar

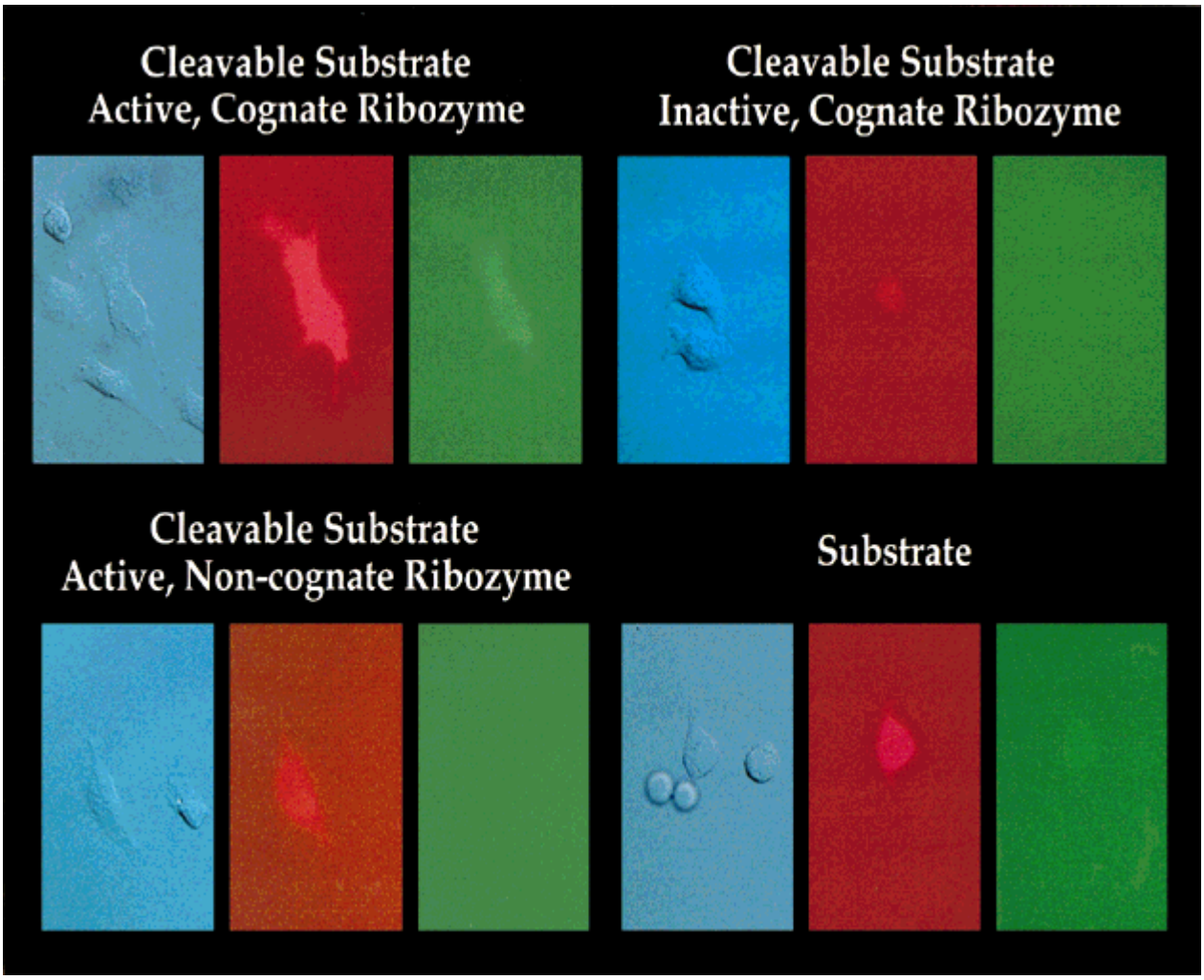

FIGURE 4. Visualization of intracellular *trans*-cleavage reactions catalyzed by the hairpin ribozyme. Representative OST-7 cells were photographed for each case under visible light transmission prior to manipulation. Microinjection was performed under visible light. Green images (blue light excitation) were photographed first 1–2 min after microinjection, then red images (green light excitation) were photographed 1 min later. The same cells are depicted under bright field, fluorescein (FRET donor, green), and tetramethylrhodamine (FRET acceptor, red) excitation.

findings were noted when the cells were irradiated intermittently after comicroinjection, with each exposure lasting no longer than 30 s at intervals of 30 s to 1 min. No change in fluorescence was observed, other than the gradual decrease in the intensity of the red signal. These findings demonstrate that the substrate is not degraded intracellularly during the time course of these experiments.

When active ribozyme was coinjected with cognate, cleavable substrate, strong disruption of energy transfer was observed (Fig. 4, upper left). Fluorescein emission was noted immediately upon excitation, although the signal was weaker than the tetramethylrhodamine emission. The signal persisted for $\leq$5 min, presumably because of photobleaching with continued exposure to the UV source. An identical fluorescence pattern was observed when precleaved substrate was injected into living cells (data not shown).

To address the possibility of a change in the FRET signal because of an antisense binding effect, we coinjected two separate populations of OST7 cells with either noncleavable substrate ($G_{+1}A$) and active ribozyme (data not shown), or with cleavable substrate with G_8A, $G_{21}U$ inactive ribozyme (Fig. 4, upper right). In each case, the FRET signal persisted for the same amount of time that was observed when the substrate was injected in the absence of ribozyme. Therefore, we conclude that formation of the ribozyme–substrate complex does not alter the in vivo FRET signal.

To investigate reaction specificity, we microinjected the substrate and a ribozyme with altered substrate specificity that is unable to cleave substrate in vitro. No

evidence of FRET disruption was observed, indicating that no cleavage occurred within the cell (Fig. 4, lower left). These data further support the conclusion that the observed change in FRET activity results from specific ribozyme-mediated intracellular cleavage of the oligoribonucleotide target.

The coinjection experiments were modified to investigate the ability of an intracellularly expressed ribozyme to cleave its target in *trans.* BHK-21 cells are an adherent fibroblast-like cell line displaying morphology and growth characteristics comparable to the OST-7 cells used in the coinjection experiments. Naive cells from this line were transfected with a vector containing a human U6 promoter cassette encoding a hairpin ribozyme and flanking stem-loops whose core sequence is identical to the one pictured in Figure 1. Cells stably expressing ribozymes were selected for further studies. Clonal cell lines expressing approximately 2,000 copies per cell (~830 pM) have been characterized in this laboratory and currently are being used for ongoing antiviral studies (A. Seyhan, D. Vitiello, M. Shields, & J.M. Burke, unpubl. data). In situ hybridization experiments suggest that the ribozymes driven by a U6 promoter are located predominantly in the nucleus (M. Shields & J.M. Burke, unpubl. observations).

We introduced only the FRET substrate into BHK-21 cell lines to determine whether intracellular ribozyme can bind and cleave its target in *trans* after substrate microinjection (Fig. 5). A 20-μM solution of double-labeled substrate in microinjection buffer was used to inject the nuclei of three different cell populations. They include naive cells; cells expressing an active, cognate ribozyme; and cells expressing an active, but noncognate ribozyme.

Substrate was injected into the nucleus of naive BHK-21 cells. Comparable to the findings in the coinjection studies, green fluorescence was not observed. However, tetramethylrhodamine fluorescence was immediate, demonstrating the substrate's presence within the cell. Nuclear tetramethylrhodamine fluorescence predominated for approximately 5 min although a low level of diffuse fluorescence was noted in the cytoplasm within 30 s after injection (Fig. 5, lower panel).

Next, we injected fluorescent substrate into cells expressing active, noncognate ribozyme. The sequence of the substrate cleavable by the constitutively expressed ribozymes differs from that of the FRET substrate by 8 of the 10 nt that form helices 1 and 2 with the substrate-binding arm of the ribozyme. Again, there was an absence of green fluorescence throughout the cell after injection. Tetramethylrhodamine fluorescence remained predominantly nuclear (Fig. 5, middle panel), lasting for approximately 5 min. These single-component microinjection experiments demonstrate that FRET decay does not occur in the absence of a ribozyme that can bind its target.

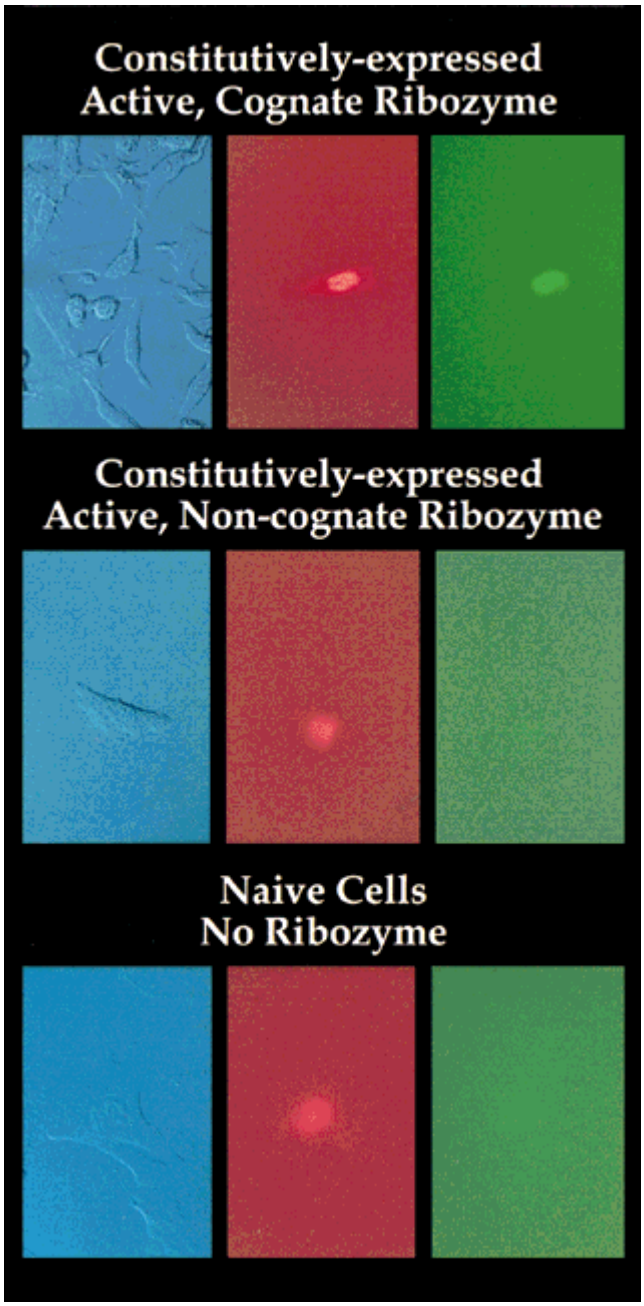

FIGURE 5. Visualization of intracellular *trans*-cleavage catalyzed by constitutively expressed hairpin ribozyme. Representative engineered or naive BHK-21 cells were photographed for each case under visible light transmission prior to manipulation. Microinjection was performed under visible light. Green images (blue light excitation) were photographed first 1–2 min after microinjection, then red images (green light excitation) were photographed 1 min later. The same cells are depicted under bright field, fluorescein (FRET donor, green), and tetramethylrhodamine (FRET acceptor, red) excitation.

Specific *trans*-cleavage activity from a constitutively expressed cognate ribozyme was demonstrated when FRET substrate was injected into the nuclei of cells that stably express ribozyme targeting this substrate. Fluorescein emission, in addition to tetramethylrhoda-

mine fluorescence, was noted immediately after injection, lasting approximately 3 and 5 min, respectively. Both fluorescence signals remained nuclear with some diffuse cytoplasmic fluorescence (Fig. 5, upper panel). These data further demonstrate that ribozyme can discriminate and cleave its target rapidly in a living mammalian cell.

DISCUSSION

Fluorescence resonance energy transfer has allowed us to visualize ribozyme-catalyzed cleavage of RNA molecules within individual cells. To our knowledge, it is the first report of direct visual monitoring of intracellular ribozyme catalysis. Our experiments indicate that requirements for binding and cleavage of substrate are the same in vivo as in vitro. Those base substitutions that prevent substrate binding or cleavage in the test tube also prevent substrate cleavage within cells as measured by the FRET assay.

Loss of FRET signal occurred within 1 min of microinjection of either substrate and ribozyme, or substrate alone into cells constitutively expressing ribozyme. Although 6 min passed before a shift in spectral dominance was demonstrated by fluorometry in vitro, the reaction between the substrate and ribozyme began immediately upon the ribozyme's addition (Fig. 2A and Table 1). There may be many reasons for different rates of FRET disruption observed in vitro and in vivo. The intracellular magnesium concentration is approximately 20 mM of which approximately 0.5 mM represents free ion (Schoolwerth et al., 1997). The low concentration of free intracellular magnesium ion may be compensated by interactions of the ribozyme complex with cellular factors (Tsuchihashi et al., 1993; Coetzee et al., 1994; Jeng et al., 1996; Sioud & Jespersen, 1996; Luzi et al., 1997; Nedbal & Sczakiel, 1997) through resolving misfolded structures (Herschlag et al., 1994), stabilizing transient, active conformers (Weeks & Cech, 1996), or colocalizing ribozyme and its target RNA.

We have demonstrated that proteins present in dialyzed cellular and nuclear extracts increase catalytic rates of the hairpin ribozyme under single-turnover conditions by a factor of six (Q. Yu & J.M. Burke, unpubl. results). The apparent acceleration of intracellular cleavage suggests that the intracellular environment may, in fact, be quite favorable for ribozyme activity. Currently, we are adding ratiometric dual-emission photometric capabilities to our microscope so that we can assess live cells in a manner comparable to fluorometry.

This work demonstrates that the *trans*-acting hairpin ribozyme can bind and cleave its target within cells. Furthermore, this intracellular FRET assay allows the tracking of ribozyme activity in short times of direct observation, providing a systematic means of optimizing ribozyme activity within an array of cell types. Maximizing the ribozyme's capacity for intracellular selectivity and specificity is essential in the development of ribozymes for targeted RNA cleavage in the laboratory or in clinical settings.

MATERIALS AND METHODS

Ribozyme preparation

Flanking stem-loop structures were cloned into ribozyme DNA constructs; RNA molecules were transcribed using T7 RNA polymerase and plasmid linearized by *Hin*dIII digestion. The 5′-flanking stem loop was derived from the bacteriophage R17 coat-protein-binding RNA stem loop from which A_9 was deleted to inhibit protein binding (Sargueil et al., 1995). A 3′-stem-loop (MacDonald et al., 1993) and self-cleaving hammerhead ribozyme were inserted immediately downstream of the ribozyme to protect the 3′ end and to ensure homogeneity of the 3′ end of the transcript (Chowrira et al., 1994).

Substrate preparation

All oligonucleotides were synthesized employing solid-phase phosphoramidite chemistry as described (Walter & Burke, 1997). Fluorescein-, 2′ O-methyl ribonucleosides-, amino-modifier-phosphoramidites (Glen Research, Virginia) and phosphorothioate linkages were incorporated at specific sites during synthesis. RNA oligoribonucleotides were deprotected and purified as described (Wincott et al., 1995; Walter et al., 1998). A succinimidyl ester of tetramethylrhodamine (Molecular Probes, Oregon) was coupled to the C_6-dT-amino-linker of the HPLC-purified fluorescein-labeled substrate according to the manufacturer's instructions. The double-labeled substrate was repurified by C_8-reverse-phase HPLC.

Trans-cleavage assays

Single-turnover cleavage assays were performed using 5′-end-labeled substrates as described, unless otherwise noted (Esteban et al., 1997). Single-turnover assays were performed on fluorescent double-labeled substrates (300 nM) as described (Walter & Burke, 1997; Walter et al., 1998). Assays were performed in a 3-mm path length cuvette at 37 °C, unless otherwise noted. Double-emission scans (peak maxima: 520 nm and 585 nm) were taken from a single-excitation wavelength of 492 nm. Both excitation and emission bandpass filters allowed $\pm$4 nm. The ratio of emissions at 585 nm to 520 nm (acceptor to donor), representing relative FRET efficiency, was calculated at 0.8-s intervals. Reactions were initiated by ribozyme addition, preincubated at 37; dgC in the same buffer.

Microinjection of fluorescent substrates

Two separate cell lines were used for microinjection experiments. OST-7 cells, a murine L-cell line (Elroy-Stein & Moss, 1990) were used for coinjection experiments and BHK-21 cells that stably express functional ribozyme (A. Seyhan, in prep.) were used for injection of substrate alone. Each cell line was cultured to 20–40% confluency on glass chamber slides. Cells were washed twice in growth media without

phenol red indicator and supplemented with 50 mM HEPES (pH 7.8). The microinjection buffer consisted of 10 mM NaH_2PO_4/Na_2HPO_4 (pH 7.2), 70 mM KCl. Double-labeled substrate (1.5 μM) and ribozyme (30 μM) were resuspended in microinjection buffer (5 μL total), centrifuged (15,000 $\times$ *g*) for 10 min, and loaded into a microinjection needle (Eppendorf, Wisconsin). Individual cells were visualized under visible light transmission. The Eppendorf transjector/micromanipulator 5171 system (Eppendorf) was used to deliver a 0.5-s pulse cytosolic injection (approximately 5–15 fL into a total cell volume of 4 pL) or a 0.5-s nuclear injection; the cell swelled momentarily upon injection.

Monitoring intracellular FRET

Fluorescence was visualized on a Nikon Eclipse TE300 inverted microscope with Nomarski imaging and epifluorescence attachments (Nikon, New York). A heat-absorbing filter in combination with a band-pass filter (630–730 nm) removed short UV and infra-red light. Fluorescein emission was monitored through a 465–495-nm excitation band-pass filter. A dichroic mirror (505 nm) removed contaminating blue excitation light from the fluorescence signal. An additional barrier-pass filter of 515 nm further filtered emitted light. There was no filter bleedthrough. Similarly, a 541–551-nm excitation band-pass filter, 575-nm dichroic mirror, and a 590-nm barrier-pass filter allowed monitoring of tetramethylrhodamine emission. A neutral density (1/8) filter decreased excitation light intensity. Images excited with 465–495 nm were photographed 1–2 min following microinjection and after observation at both excitation wavelengths. Photographs of tetramethylrhodamine emission were taken 2–3 min after microinjection.

ACKNOWLEDGMENTS

We would like to thank Nils Walter, Gary Ward, Harm J. Knot, Robert Pinard, Qiao Yu, Attila Seyhan, and Joyce Heckman for their assistance during experimentation and during manuscript preparation, and Attila Seyhan for stably expressing cell lines. This work was supported by grants from the National Institute of Allergy and Infectious Diseases and the National Institutes of Health to J.M.B.

Received May 12, 1999; returned for revision June 8, 1999; revised manuscript received February, 2000

REFERENCES

Beck J, Nassal M. 1995. Efficient hammerhead ribozyme-mediated cleavage of the structured hepatitis B virus encapsidation signal in vitro and in cell extracts, but not in intact cells. *Nucleic Acids Res 23*:4954–4962.

Beigelman L, McSwiggen JA, Draper KG, Gonzalez C, Jensen K, Karpeisky AM, Modak AS, Jasenka MA, DiRenzo AB, Haeberli P, Sweedler D, Tracz D, Grimm S, Wincott FE, Thackray VG, Usman N. 1995. Chemical modifications of hammerhead ribozymes. *J Biol Chem 27*:25702–25708.

Bertrand E, Pictet R, Grange T. 1994. Can hammerhead ribozymes be efficient tools to inactivate gene function? *Nucleic Acids Res 22*:293–300.

Berzal-Herranz A, Joseph S, Chowrira B, Butcher S, Burke JM. 1993. Essential nucleotide sequences and secondary structure elements of the hairpin ribozyme. *EMBO J 12*:2567–2574.

Birikh K, Heaton P, Eckstein F. 1997. The structure, function and application of the hammerhead ribozyme. *Eur J Biochem 245*:1–16.

Borneman J, Tritz R, Hampel A, Altschuler M. 1995. Detection of cleavage products from an in vivo transcribed *cis* hairpin ribozyme in turnips using the CaMV plant virus. *Gene 159*:137–142.

Burke JM. 1996. Hairpin ribozyme: Current status and future prospects. *Biochem Soc Trans 24*:608–615.

Chowrira B, Berzal-Herranz A, Burke JM. 1991. Novel guanosine requirement for catalysis by the hairpin ribozyme. *Nature 354*:320–322.

Chowrira B, Berzal-Herranz A, Burke JM. 1993. Ionic requirements for RNA binding, cleavage, and ligation by the hairpin ribozyme. *Biochemistry 32*:1088–1095.

Chowrira B, Pavco P, McSwiggen J. 1994. In vitro and in vivo comparison of hammerhead, hairpin, and hepatitis delta virus self-processing ribozyme cassettes. *J Biol Chem 269*:25856–25864.

Christoffersen RE, Marr JJ. 1995. Ribozymes as human therapeutic agents. *J Med Chem 38*:2023–2037.

Clegg R. 1992. Fluorescence resonance energy transfer and nucleic acids. *Methods Enzymol 211*:353–389.

Coetzee T, Herschlag D, Belfort M. 1994. *Escherichia coli* proteins, including ribosomal protein S12, facilitate in vitro splicing of phage T4 introns by acting as RNA chaperones. *Genes & Dev 8*:1575–1588.

Crisell P, Thompson S, James W. 1993. Inhibition of HIV-1 replication by ribozymes that show poor activity in vitro. *Nucleic Acids Res 21*:5251–5255.

Domi A, Beaud G, Favre A. 1996. Transcripts containing a small anti-HIV hammerhead ribozyme that are active in the cell cytoplasm but inactive in vitro as free RNAs. *Biochimie 78*:654–662.

Donahue C, Fedor M. 1997. Kinetics of hairpin ribozyme cleavage in yeast. *RNA 3*:961–973.

Earnshaw D, Gait M. 1997. Progress toward the structure and therapeutic use of the hairpin ribozyme. *Antisense Nucleic Acid Drug Dev 7*:403–411.

Elroy-Stein O, Moss B. 1990. Cytoplasmic expression system based on constitutive synthesis of bacteriophage T7 RNA polymerase in mammalian cells. *Proc Natl Acad Sci USA 87*:6743–6747.

Esteban JA, Banerjee AB, Burke JM. 1997. Kinetic mechanism of the hairpin ribozyme. *J Biol Chem 272*:13629–13639.

Heidenreich O, Xy X, Nerenberg M. 1996. A hammerhead ribozyme cleaves its target RNA during RNA preparation. *Antisense Nucleic Acid Drug Dev 6*:141–144.

Herschlag D, Kholsa M, Tsuchihashi Z, Karpel R. 1994. An RNA chaperone activity of non-specific RNA binding proteins in hammerhead ribozyme catalysis. *EMBO J 13*:2913–2924.

Jeng KS, Su PY, Lai MM. 1996. Hepatitis delta antigens enhance the ribozyme activities of hepatitis delta virus RNA in vivo. *J Virol 70*:4205–4209.

Jones JT, Lee SW, Sullenger BA. 1996. Tagging ribozyme reaction sites to follow trans-splicing in mammalian cells. *Nat Med 26*:643–648.

Jones JT, Sullenger BA 1997. Evaluating and enhancing ribozyme reaction efficiency in mammalian cells. *Nat Biotechnol 15*:902–905.

Kohler U, Ayre BG, Goodman HM, Haseloff J. 1999. Trans-splicing ribozymes for targeted gene delivery. *J Mol Biol 285*:1935–1950.

Lieber A, Strauss M. 1995. Selection of efficient cleavage sites in target RNAs by using a ribozyme expression library. *Mol Cell Biol 15*:540–551.

Luzi E, Eckstein F, Barbacchi G. 1997. The newt ribozyme is part of a riboprotein complex. *Proc Natl Acad Sci USA 94*:9711–9716.

MacDonald LE, Zhou Y, McAllister W. 1993. Termination and slippage by bacteriophage T7 RNA polymerase. *J Mol Biol 232*:1030–1047.

Nedbal W, Sczakiel G. 1997. Hammerhead ribozyme activity in the presence of low molecular weight cellular extract. *Antisense Nucleic Acid Drug Dev 7*:585–589.

Perkins T, Goodchild J. 1997. Using fluorescence resonance energy transfer to investigate hammerhead ribozyme kinetics. *Meth Mol Biol 74*:241–251.

Perkins T, Wolf D, Goodchild, J. 1996. Fluorescence resonance energy transfer analysis of ribozyme kinetics reveals the mode of

action of a facilitator oligonucleotide. *Biochemistry 35*:16370–16377.
Rossi J. 1997. Therapeutic applications of catalytic antisense RNAs (ribozymes*). Ciba Found Symp 209*:195–206.
Sargueil B, Pecchia D, Burke JM. 1995. An improved version of the hairpin ribozyme functions as a RNP Complex. *Biochemistry 34*:7739–7748.
Schoolwerth A, Feldman G, Culpepper R. 1997. *Textbook of internal medicine*. 3rd ed. Philadelphia: Lippincott-Raven Press.
Seyhan A, Amaral J, Burke JM. 1998. Intracellular RNA cleavage by the hairpin ribozyme. *Nucleic Acids Res 26*:3494–3504.
Sioud M, Jespersen L. 1996. Enhancement of hammerhead ribozyme catalysis by glyceraldehyde-3-phosphate dehydrogenase. *J Mol Biol 257*:775–789.
Sixou S, Szoka F, Green G, Glusti B, Zon G, Chin D. 1994. Intracellular oligonucleotide hybridization detected by fluorescence resonance energy transfer (FRET). *Nucleic Acids Res 22*:662–668.
Steinecke P, Steger G, Schreier PH. 1994. A stable hammerhead structure is not required for endonucleolytic activity of a ribozyme in vivo. *Gene 149*:47–54.
Sullenger BA, Cech TR. 1994. Ribozyme-mediated repair of defective mRNA by targeting *trans*-splicing. *Nature 371*:619–622.
Sun LQ, Warrilow D, Wang L, Witherington C, MacPhearson J, Symonds G. 1994. Ribozyme-mediated suppression of Moloney murine leukemia virus and human immunodeficiency virus type I replication in permissive cell lines. *Proc Natl Acad Sci USA 91*:9715–9719.
Tsuchihashi Z, Kholsa M, Herschlag D. 1993. Protein enhancement of hammerhead ribozyme catalysis. *Science 262*:99–102.
Uchiyama H, Hirano K, Masaki K, Taira K. 1996. Detection of undegraded oligonucleotides in vivo by fluorescence resonance energy transfer. *J Biol Chem 271*:380–384.
Walter N, Albinson E, Burke JM. 1997. Probing structure formation in the hairpin ribozyme using fluorescent substrate analogs. *Nucleic Acids Symp Ser 36*:175–177.
Walter N, Burke JM. 1997. Real-time monitoring of hairpin ribozyme kinetics through base-specific quenching of fluorescein-labeled substrates. *RNA 3*:392–404.
Walter N, Hampel K, Brown K, Burke JM. 1998. Tertiary structure formation in the hairpin ribozyme monitored by fluorescence resonance energy transfer. *EMBO J 17*:2378–2391.
Weeks KM, Cech TR. 1996. Assembly of a ribonucleoprotein catalyst by tertiary structure capture. *Science 271*:345–348.
Welch PJ, Tritz R, Yei S, Leavitt M, Yu M, Barber J. 1996. A potential therapeutic application of hairpin ribozymes: In vitro and in vivo studies of gene therapy for hepatitis C virus infection. *Gene Ther 3*:994–1001.
Wincott F, DiRenzo A, Shaffer C, Grimm S, Tracz D, Workman C, Sweedler D, Gonzalez C, Scaringe S, Usman N. 1995. Synthesis, deprotection, analysis and purification of RNA and ribozymes. *Nucleic Acids Res 23*:2677–2684.
Yu Q, Pecchia DB, Kingsley SL, Heckman JE, Burke JM. 1998. Cleavage of highly structured viral RNA molecules by combinatorial libraries of hairpin ribozymes. *J Biol Chem 273*:23524–23533.